FLIGHT TEST DERIVED HEATING MATH MODELS FOR CRITICAL LOCATIONS ON THE ORBITER DURING REENTRY

Elam K. Hertzler and Paul W. Phillips
Air Force Flight Test Center
Edwards Air Force Base, California

INTRODUCTION

An analysis technique was developed for expanding the aerothermodynamic envelope of the Space Shuttle orbiter without subjecting the vehicle to sustained flight at more stressing heating conditions. A transient analysis program was developed to take advantage of the transient maneuvers that were flown as part of this analysis technique. This program derived heat rates from flight test data for various locations on the orbiter. The flight-derived heat rates were used to update heating models based on predicted data. Future missions were then analyzed based on these flight-adjusted models.

This paper will present a technique for comparing flight and predicted heating-rate data and the extrapolation of the data to predict the aerothermodynamic environment of future missions.

ABBREVIATIONS AND SYMBOLS

AFFTC	Air Force Flight Test Center
deg F	degrees Fahrenheit
FRSI	Flexible Reusable Surface Insulation
HRSI	High Temperature Reusable Surface Insulation
KSC	Kennedy Space Center
LRSI	Low Temperature Reusable Surface Insulation
NASA	National Aeronautics and Space Administration
OMS	Orbital Maneuvering System
POPU	pushover-pullup
q	heating rate
q_{ref}	reference heating rate
Re_∞	free-stream Reynolds number
RTV	Room Temperature Vulcanized
STS-1,2,3,4,5	Space Transportation System flights 1, 2, 3, 4, and 5
TPS	Thermal Protection System

VAFB	Vandenberg AFB
X/L	longitudinal location nondimensionalized by the orbiter reference length
α	angle of attack, degrees
β	sideslip angle, degrees
δBF	bodyflap deflection, degrees
δe	elevator deflection, degrees

ANALYSIS TECHNIQUE

An analysis technique was developed (Figure 1) that allows accurate predictions of the aerothermodynamic environment of the Space Shuttle orbiter for future missions. Locations or control points were chosen based on the original NASA preflight selected control points (but at locations where temperature instrumentation was available) and the problem areas highlighted through analysis of wind tunnel data. A transient maneuver was designed where the Shuttle commander manually reduced the angle of attack of the orbiter to a predetermined point and then increased the angle of attack above the nominal (pushover-pullup (POPU)) so as to balance out the energy state of the orbiter. A transient analysis program was developed by the AFFTC that determined the change in the heating rate (nondimensionalized by a reference heating rate) with respect to angle of attack, sideslip, elevon deflection, or body flap deflection during the POPU maneuver. The transient analysis program utilized the actual flight trajectory, atmosphere, flight thermocouple data, one-dimensional thermal model, and material properties (Reference 1). An independent analysis program was also developed at the AFFTC that derived heat rates from the flight surface thermocouple data using an equilibrium temperature assumption and an empirically derived time constant in an algorithm which approximated the thermal properties of the coating. These two programs were applied to the flight data to update heating models for the AFFTC's control points which were originally based on both NASA contractor heating models and wind-tunnel-derived heating models. The final goal of this analysis was to use these flight-adjusted models to predict the surface and bondline temperatures for future missions. The predictions were calculated using a trajectory from a six-degree-of-freedom engineering simulator at the AFFTC and a one-dimensional thermal model.

This paper will not deal with the rigorous mathematical and statistical details of the computer programs utilized in this analysis. For details of this nature see References 2 and 3.

MATH MODELS

The AFFTC maintains nine thermodynamic math models, considered to be the most critical instrumented locations (control points), for the purpose of assessing the orbiter's ability to handle future missions. Figure 2 shows the locations of the various control points and their respective Thermal Protection System (TPS) materials along with the original NASA control points for comparison.

Lower Surface

The AFFTC heating math model on the centerline at X/L = 0.02 was originally comprised of the NASA contractor simplified heating model (Figure 3). The parameter estimation program was not utilized at this location due to the small response to angle of attack (as predicted) during the POPU maneuvers flown on STS-2, STS-4, and STS-5. The independent analysis program was used to obtain laminar heating levels for this location. The heating model was found to be conservative and was updated by reducing the heating levels by approximately 14 percent (Figure 4). Note that the flight-adjusted heating model matched the flight data quite well.

The AFFTC heating math model located on the centerline at X/L = 0.7 was originally the NASA contractor simplified heating model. The results from the transient analysis program for the STS-2 Mach 21 POPU dynamic test maneuver indicated that the laminar heating levels of the original heating model were conservative. The heating model was adjusted by reducing the laminar levels by approximately 14 percent. Additionally, the boundary layer transition in flight occurred at a higher Reynolds number (later in the entry) than predicted. Figure 5 shows a graphical representation of the original and flight-adjusted heating models. The independent analysis program was used to adjust the transitional and turbulent heating levels. The flight-adjusted heating model then provided a good comparison with flight data (Figure 6).

An off-centerline location at X/L = 0.7 was added which was more critical for missions with higher heat loads due to the thinness of the High Temperature Reusable Surface Insulation (HRSI) tiles in this region leading to increased bondline temperatures. (Bondline refers to the inner bondline which is representative of the structural skin temperature.) Similar methods of updating the heating model were applied to this location.

The AFFTC elevon control point was located at the left-hand outboard elevon tip and was originally based on a NASA contractor simplified heating model. Both the simplified and flight-adjusted heating models are graphically represented in Figure 7 (shown at zero deflection angle for simplicity). The model was updated with flight data results from both analysis programs. Figure 8 indicates how the original temperature predictions for STS-2 and those from the flight-adjusted model compare to the actual flight data. The actual transition occurred at a higher Reynolds number (i.e., later in the flight) than was the case for the original prediction.

The AFFTC body flap control point was located at the body flap edge and was based on the laminar portion of the NASA contractor simplified heating model for the centerline location. The simplified heating model contained information for body flap deflection angles of less than 15 degrees. Wind-tunnel-derived data was added to the flight-adjusted heating model in order to extend the model to body flap deflection angles of 22.5 degrees. The body flap edge location was chosen due to the consistently higher temperatures observed in the flight data when compared to the centerline thermocouple. Figure 9 indicates the adjustments made to the heating model utilizing results from the independent analysis program to extrapolate the laminar heating levels to the transitional and turbulent levels. The Mach 17 body flap sweep on STS-2 indicated an interaction between heating on the body flap and the elevon deflection angle. This phenomenon has not been incorporated into the model at

present due to insufficient data. Figure 10 is the time history of the bodyflap edge thermocouple for STS-2 compared with predictions. The flight data indicated that the flow over the body flap may have been in a transitional/turbulent state for a large portion of the reentry before becoming fully turbulent. The original prediction of a rapid onset of boundary layer transition is obvious on this plot.

Results for the bondline temperatures at the X/L = 0.7 centerline location did not compare with flight test bondline measurements (Figure 11). One contributing factor was the late transition to turbulent flow, which led to a lower overall heat load. It was also determined that after the payload bay vent doors opened at Mach 2.5, the cool, atmospheric air allowed convective cooling to occur internally, which dissipated the heat soaking through to the backface of the structure, thereby reducing the bondline temperatures. (Backface refers to the back side of the substructure.) Additionally, the internal structure was cool enough to allow reradiation from the backface. Both the elevon tip and body flap edge were passively vented and were therefore subject to the free convective cooling effects. The lower backface of the control surfaces apparently radiated to the cooler backface of the upper surface. Terms to account for the free convective and radiative effects were applied to the one-dimensional thermal models for the fuselage and control surface control points. After the adjustments to the heating model were implemented, the bondline prediction for X/L = 0.62 was close to the actual flight data so the cooling effects were not applied.

Upper Surface

Two control points are located on the left Orbital Maneuvering System (OMS) pod (Figure 2). Postflight inspections have indicated that there are other problem areas on the upper surface (Reference 4) that will need to be modeled, but to date the OMS pod has received the most attention.

The aft OMS pod control point is located on the Flexible Reusable Surface Insulation (FRSI) at thermocouple V07T9976A. The wind-tunnel-derived and flight-adjusted heating models are shown on Figure 12. Figure 13 is a comparison of the thermocouple time history and predicted thermocouple response based on the heating models. A large discrepancy in the wind-tunnel-derived heating model and flight data was highlighted by the Mach 20 POPU maneuver indicated on Figure 13. The heating on the OMS pod is a function of angle of attack due to a vortex created at the wing glove area of the forward fuselage. (The heating is also dependent on Reynolds number and sideslip but to a lesser extent than angle of attack.) Specifically, as the angle of attack is reduced from the nominal 40 degree value, the vortex impinges on the OMS pod. Analysis of the wind tunnel data indicated that the impingement would occur abruptly at 30 degrees angle of attack, whereas the flight thermocouple data indicated that impingement began at about 37 degrees. Also, the effect of Reynolds number on the actual heating level due to the vortex impingement was underpredicted by the wind-tunnel-derived results. POPU maneuvers on flights two and four were analyzed with the parameter estimation program and the results were used to create the flight-adjusted model. Where flight data were not available, the flight-adjusted model was extrapolated based on trends.

Below 23 degrees angle of attack (Figure 12), the heating rate rapidly approaches the reference value (q/q_{ref} approaches 1) indicating attached flow conditions around

the OMS pods. The yaw jet interaction effects were observed to disappear (Reference 5) at about the same flight condition, further supporting the likelihood of attached flow. The irregular shapes of the OMS pod heating models are probably related to sideslip effects rather than true irregularities with angle of attack as shown in the figure. There are insufficient data available at this time to separate and identify the angle of attack and sideslip effects.

The forward OMS pod control point was a recent development that was necessary in order to evaluate proposed changes to the OMS pod TPS. This location is on the Low Temperature Reusable Surface Insulation (LRSI) at thermocouple V07T9220A on OV-102. The heating model to date is adequate for a nominal 40-degree trajectory. However, for extrapolating to future missions more flight test information will be necessary to improve confidence.

The bondline temperatures for the OMS pod control points cannot be verified due to the absence of bondline instrumentation in these areas. The cooling effects applied to the lower surface were not felt to be appropriate for the OMS pod due to the existence of a thermal blanket behind the graphite epoxy structure.

Wing Leading Edge and Nose Cap

AFFTC wing leading edge and nose cap control points are located on the reinforced carbon-carbon wing leading edge (55 percent semispan) and the nose cap respectively. Both locations used the NASA contractor simplified heating models.

The wing leading edge control point simplified heating model is represented graphically in Figure 14. The models are considered to be of low confidence due to an inability to accurately model the three-dimensional aspects of the material and uncertainty in the interpretation of the flight test instrumentation. The close match between flight data and predictions shown in Figure 15 may, therefore, be fortuitous and no updating of the carbon/carbon heating models has been attempted.

The nose cap control point is not presented graphically since only one flight (STS-5) contained valid radiometer data from the nose cap. There is low confidence in the model due to the uncertainties discussed above (under the leading edge control point). In addition, the data from flight five indicated that the maximum heating was at the stagnation point on the nose cap instead of the sonic line where it was predicted to occur. Further attention is required in the future to produce high confidence math models of carbon/carbon material and to improve flight instrumentation so that valid comparisons can be made.

FUTURE MISSIONS

Flight test data to date have been used for the formation and/or updating of heating and thermal models for the orbiter TPS and aerothermal environment. However, the data have been limited due to the limited number of POPU maneuvers available and due to recorder malfunctions (STS-1, STS-4, and STS-5). In order for a high-confidence aerothermal model to be fully developed, additional reentry test maneuvers on an instrumented orbiter are needed. Design of future vehicles will benefit from a thorough understanding of angle of attack and Reynolds number effects

on aerothermodynamic heating, especially for the upper surface. The maneuvers flown to date are indicated in Figure 15 along with the range of angle of attack capability required for operational flights. The lower angles of attack profile is associated with high crossrange entries like that required for an abort once around to Vandenberg AFB (VAFB). There is a lack of data below 30 degrees angle of attack and also between a Reynolds number of 5×10^6 and 15×10^6 which is extremely critical to the upper surface, specifically the OMS pods.

Figure 17 presents predicted surface and bondline temperatures for future reentries to both Kennedy Space Center (KSC), Florida, and VAFB, California. It is immediately obvious that the OV-102 OMS pod TPS is inadequate for any mission presented other than a 40-degree-angle-of-attack mission (nominal) Adequate margins exist at all other control points. AFFTC leading edge and nose cap points are of low confidence due to the uncertainties discussed earlier (nose cap prediction not presented).

There are other areas of concern that have not been dealt with by the AFFTC and are not subject matter of this report; for example, gap heating and tile slumping. Reference 4 presents more details.

LESSONS LEARNED

The reentry aerothermodynamic lessons learned are: windward-side heating predictions were conservative due to the combined effect of lower laminar heating levels, later-than-predicted transition to turbulent flow, and external atmospheric cooling. Structural peak temperatures were further reduced due to internal radiative and convective cooling. Leeside OMS pod heating, on the other hand, was underpredicted. Vortex impingement on the OMS pod occurred at a higher angle of attack than predicted (37 degrees rather than 30 degrees), and the unimpinged heating levels at 40 degrees angle of attack were higher than predicted.

CONCLUDING REMARKS

A flight test technique was developed and successfully used to verify predictive methods as well as select and update entry heating models. Discrepancies in heating predictions were identified. Basically, overprediction of windward-side heating and underprediction of leeside OMS pod heating were observed. The AFFTC flight test revised models have produced a good match of the respective test data for the first five orbital flights. High-confidence aerothermal models, particularly for the OMS pod, will require additional reentry heating flight test data. Design of future vehicles will benefit from continued orbiter testing through a thorough understanding of angle-of-attack and Reynolds number effects on aerothermodynamic heating, particularly on the upper surface.

REFERENCES

1. Space Shuttle Program Thermodynamic Design Data Book TPS Acreage Methods Validation, SD73-SH-0226, Volume 2, Book IIE, Rockwell International, Space Systems Group, Downey, CA, October 1981.

2. Hodge, J.K., Audley, D.R., Phillips, P.W., and Hertzler, E.R., Aerothermodynamic Flight Envelope Expansion for a Manned Lifting Reentry Vehicle (Space Shuttle), Flight Mechanics Symposium on Ground Flight Test Techniques and Correlation, Paper No. 3-A, AGARD CP-334, October 1982.

3. Hodge, J.K. and Audley, D.R., Aerothermodynamic Parameter Estimation from Space Shuttle Thermocouple Data During Transient Flight Test Maneuvers, 21st Aerospace Sciences Meeting, AIAA-83-0482, January 1983.

4. Hodge, J.K., Trends in Shuttle Entry Heating from the Correlation of Flight Test Maneuvers, Shuttle Performance: Lessons Learned, NASA CP-2238, Part 2, 1983, pp. 687-702.

5. Kirsten, P.W., Richardson, D.F., and Wilson, C.M., Predicted and Flight Test Results of the Performance, Stability, and Control of the Space Shuttle from Reentry to Landing, NASA CP-2283, Part 1, 1983, pp. 509-525.

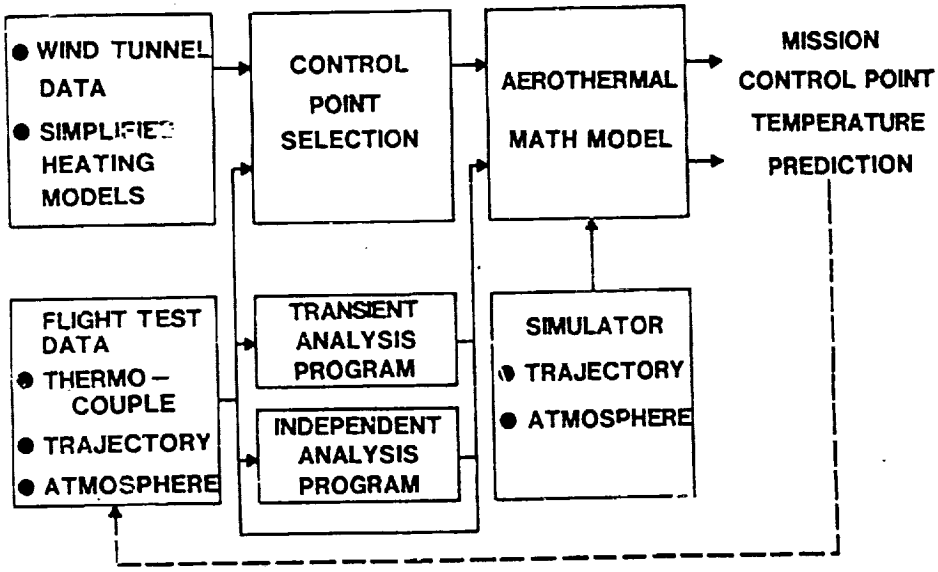

Figure 1.- Analysis technique.

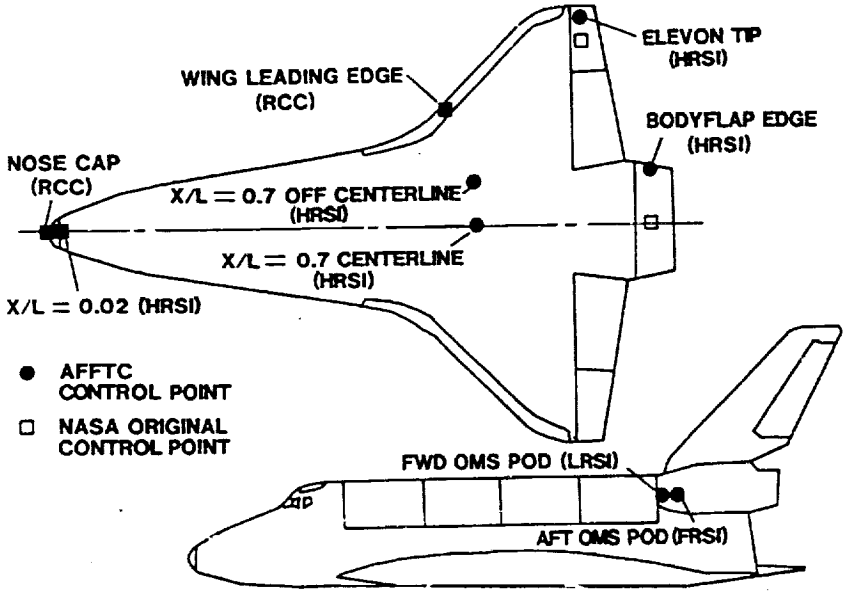

Figure 2.- Temperature control points.

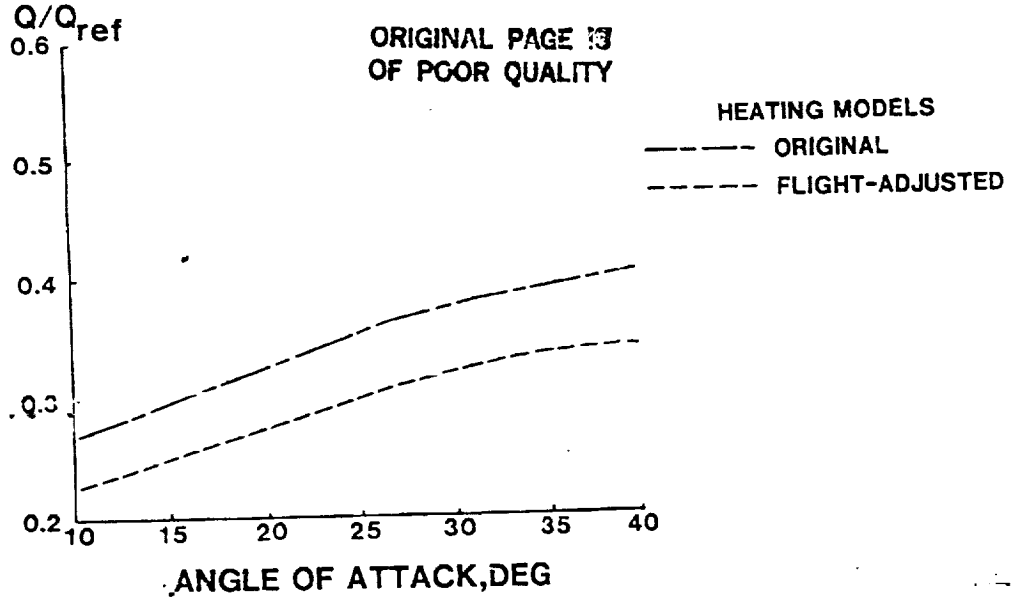

Figure 3.- Lower-surface heating model - forward location (X/L = 0.02).

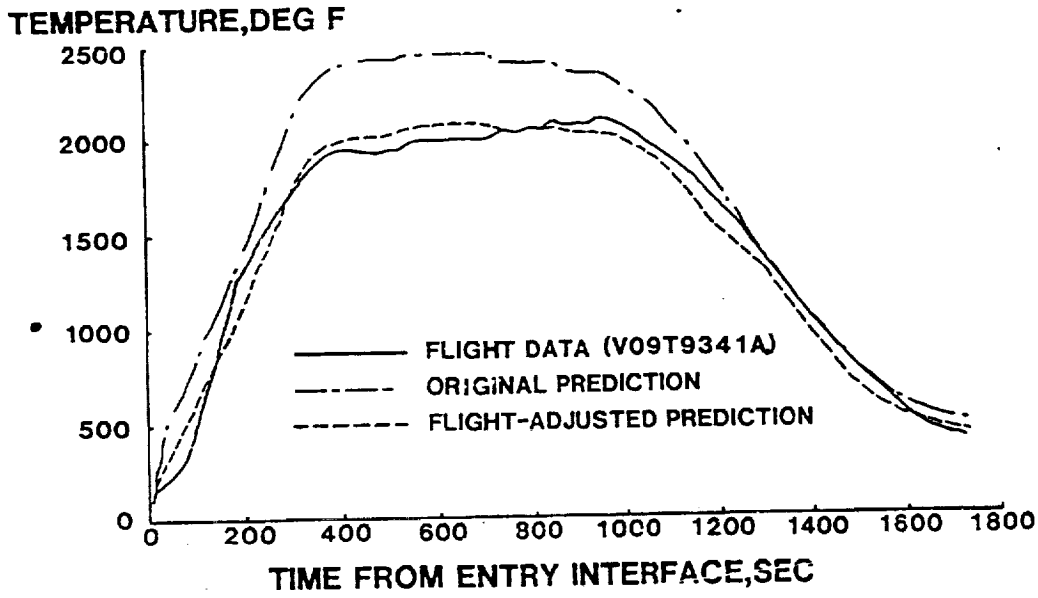

Figure 4.- Lower-surface temperature comparison - forward location (X/L = 0.02). STS-2.

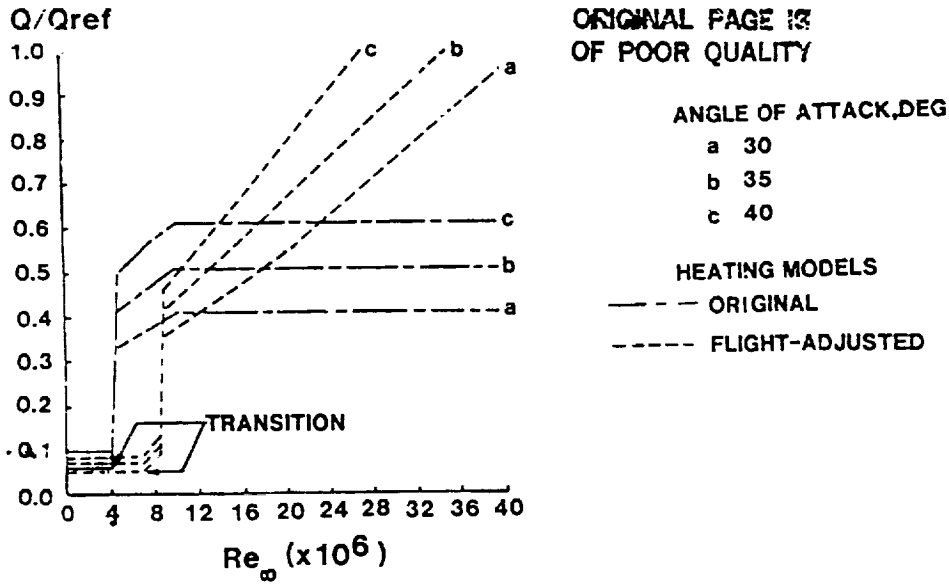

Figure 5.- Lower-surface heating model - aft location (X/L = 0.7 centerline).

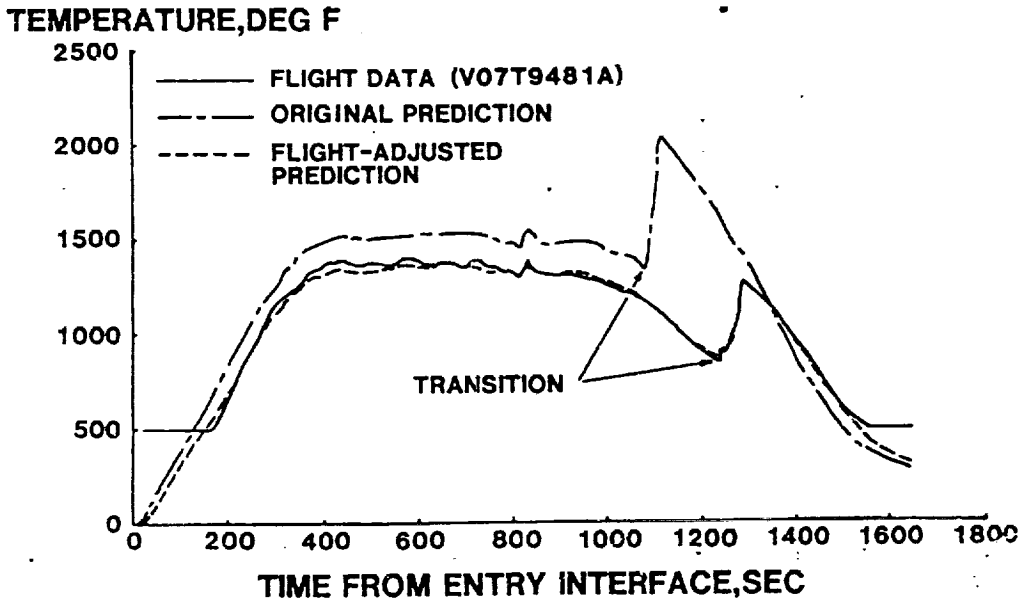

Figure 6.- Lower-surface temperature comparison - aft location (X/L = 0.7 centerline). STS-2.

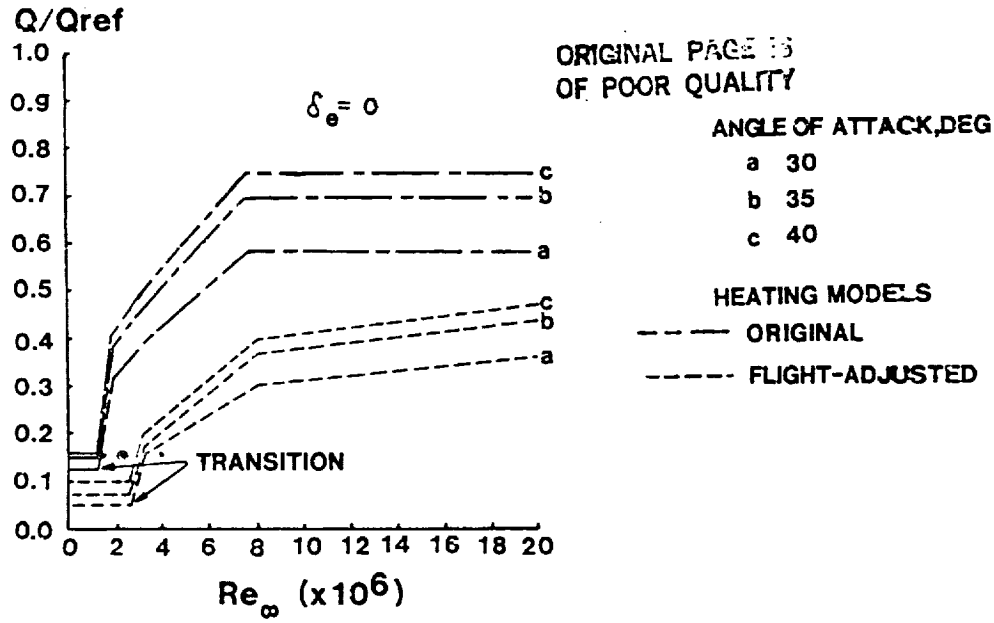

Figure 7.- Control surface heating model - elevon tip.

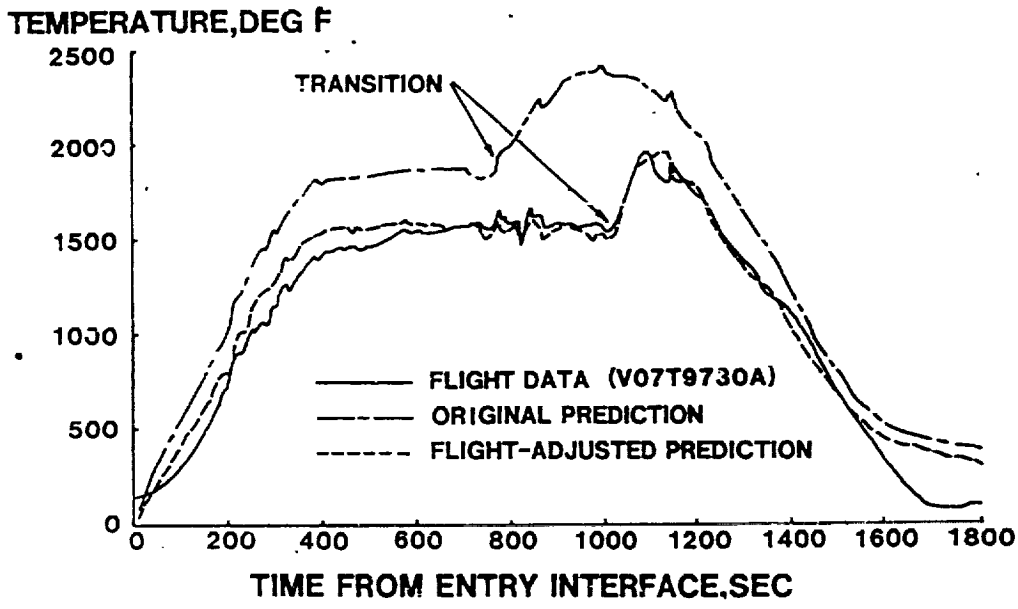

Figure 8.- Control surface temperature comparison - elevon tip. STS-2.

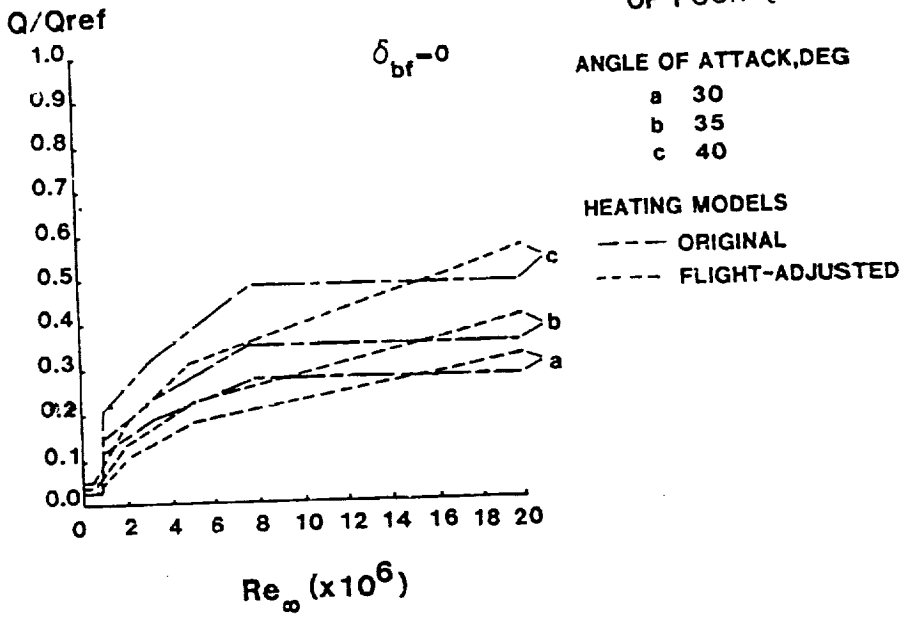

Figure 9.- Control surface heating model - bodyflap edge.

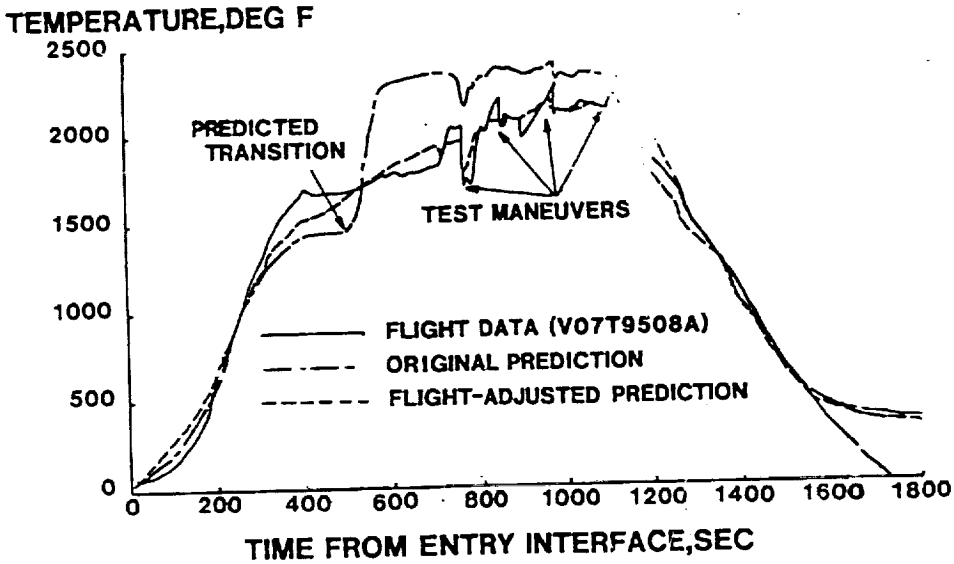

Figure 10.- Control surface temperature comparison - bodyflap edge. STS-2.

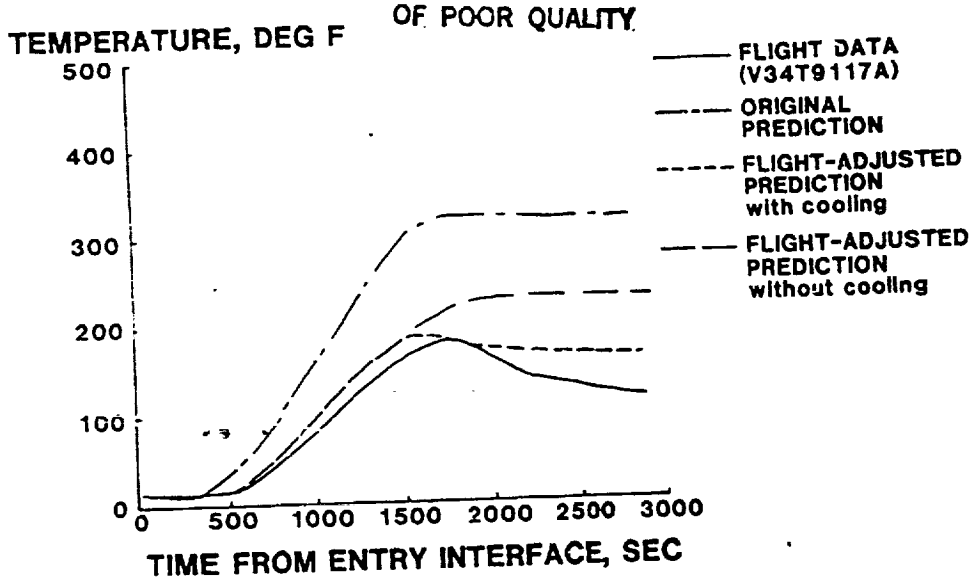

Figure 11.- Lower-surface bondline temperature comparison - aft location (X/L = 0.7 centerline). STS-2.

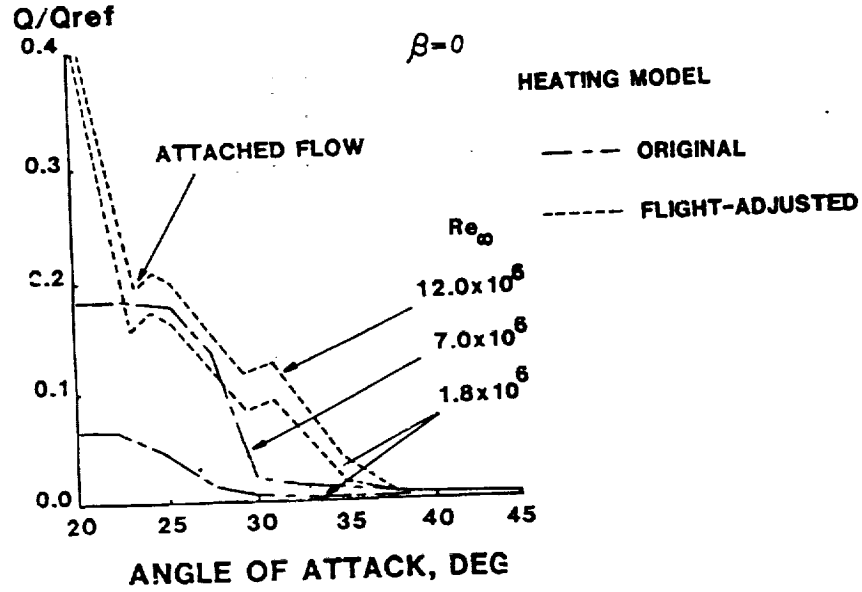

Figure 12.- OMS pod heating model - aft location.

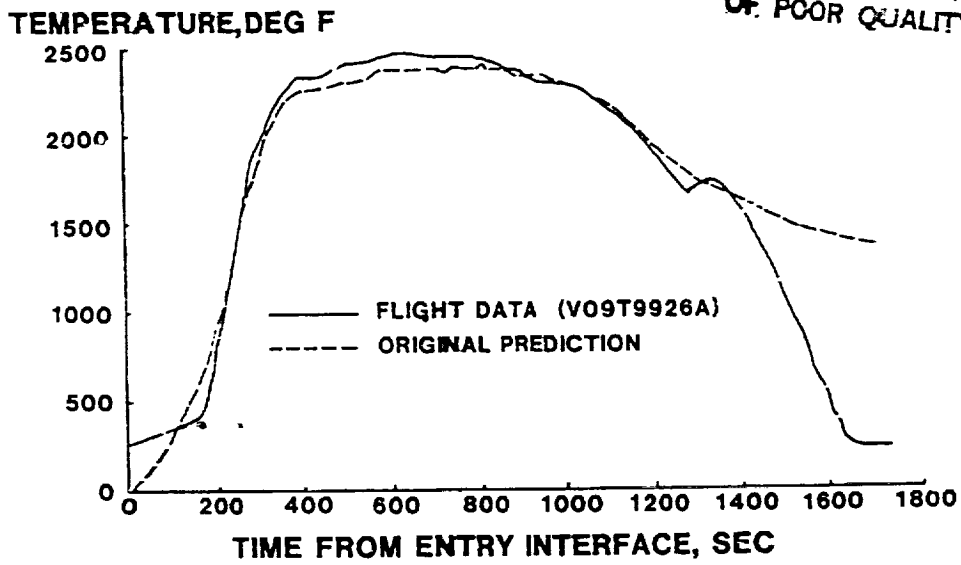

Figure 15.- Wing leading-edge temperature comparison - 55 percent semispan location. STS-2.

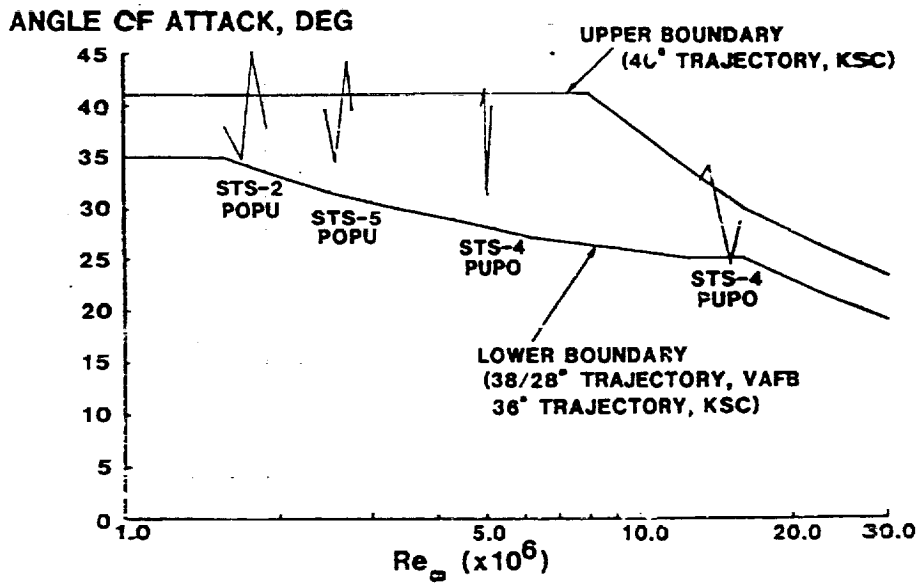

Figure 16.- Operational angle-of-attack envelope.

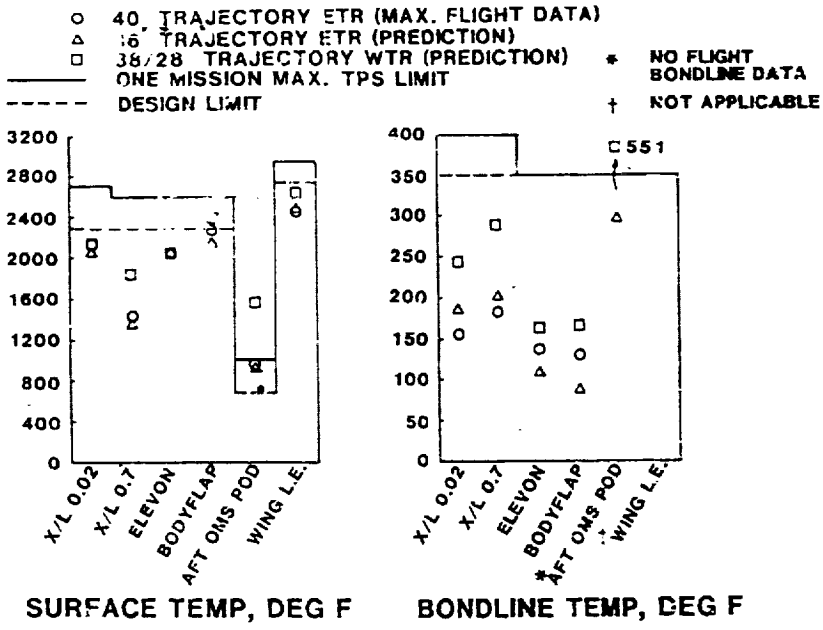

Figure 17.- Maximum temperature comparison.